A REFINEMENT OF THE ANALYTIC FUNCTION EXPANSION NODAL METHOD WITH TRANSVERSE GRADIENT BASIS FUNCTIONS AND INTERFACE FLUX MOMENTS

Sweng Woong Woo and Nam Zin Cho
Korea Advanced Institute of Science and Technology
Department of Nuclear Engineering
373-1 Kusong-dong, Yusong-gu
Taejon, Korea 305-701
k097wsw@kins.re.kr; nzcho@sorak.kaist.ac.kr

Jae Man Noh
Korea Atomic Energy Research Institute
150 Dukjin-dong, Yusong-gu
Taejon, Korea 305-353
jmnoh@nanum.kaeri.re.kr

ABSTRACT

A refinement of the Analytic Function Expansion Nodal (AFEN) method has been performed by increasing the number of flux expansion terms in the manner that the original basis functions are combined with the transverse-direction linear functions. In this manner, the added terms can render the flux expansion more complete and be kept to still satisfy the diffusion equation. The additional constraints required are provided by the interface flux moments defined as the weighted-average fluxes at the interface.

The refined AFEN method was tested against the OECD-L336 MOX benchmark problem for rectangular geometry and the VVER-440 benchmark problem for hexagonal geometry. The results show that the method improves not only the accuracy in predicting the flux distribution but also the computing time, and that it can replace the corner-point fluxes with the interface moments without accuracy degradation. The possibility of excluding the corner-point fluxes increases the flexibility in implementing this method into the existing codes that do not have the corner-point flux scheme and may make it fit better for the non-linear scheme based on two-node problems.

I. Introduction

The Analytic Function Expansion Nodal (AFEN) method has been developed and successfully applied to the analyses of the reactor cores in both rectangular and hexagonal geometries.[1-3] The success of the AFEN method is attributed to its accuracy in solving the nodal diffusion equations and its flexibility in treating various geometries appearing in the usual reactor analysis. The main feature of the AFEN method is that it expands the solution of the multidimensional diffusion equation in each node into the non-separable analytic basis functions which satisfy the diffusion equation everywhere in the node. Expanding the intranodal flux into the functions satisfying the diffusion equation locally guarantees the accuracy of the AFEN method.

In this paper, a refinement of the AFEN method is proposed to improve the accuracy further so that it should satisfy the potential demand requiring very high accuracy in both the nodal calculation and the pin-flux reconstruction calculation and to widen the spectrum of its implementations to various existing nodal codes. This refinement is performed by adding basis functions to the original flux expansion. The added functions are the products of the trigonometric functions (or the hyperbolic trigonometric functions) in a direction and possible combinations of the linear functions in the transverse directions to the direction of the trigonometric function (e.g., $y\sin(kx)$, $z\sin(kx)$, and $yz\sin(kx)$). They also satisfy the diffusion equation at any point in the node. The additional constraints required by the added terms are the continuity conditions of the flux moments and the current moments at the interfaces. These interface moments are defined by the interface-average fluxes weighted by the odd functions in the parallel directions to the interface (e.g., averages of $y\phi(x,y,z)$, $z\phi(x,y,z)$, and $yz\phi(x,y,z)$ over y and z at an interface perpendicular to the x axis). A simple choice of the weighting function is a step or a linear function with alternating sign about the center of the interface. If we choose the step function as a weighting function of the interface flux moment, the method is equivalent to the one that applies the flux and current continuity conditions at each quadrant of an interface. Since the refined flux expansion also satisfies the diffusion equation and the additional constraints are applied, the salient feature of the original AFEN method is even more enforced in the refined method.

By including the flux moments, we may eliminate the corner-point fluxes in the nodal unknowns without accuracy degradation. Excluding the corner-point fluxes may reduce the efforts required in implementing this method into the existing nodal codes that use only the node-average flux and the interface quantities as unknowns. This can also eliminate the difficulties involved in the non-linear iterative scheme of the original AFEN method induced by the edge fluxes. This version of the AFEN method seems to fit better for the non-linear scheme based on two-node problems that are solved for the interface quantities of the two nodes and is expected better performance.

II. Methodology

II.A. Rectangular Geometry

II.A.1 Intranodal Flux Expansion

To expand the intranodal homogeneous flux of a three-dimensional node into analytic basis functions, consider the three-dimensional multigroup diffusion equation in node n:

$$-\mathbf{D}^n\nabla^2\hat{\boldsymbol{\phi}}^n(\mathbf{r})+\boldsymbol{\Sigma}^n\hat{\boldsymbol{\phi}}^n(\mathbf{r})=\frac{1}{k_{eff}}\boldsymbol{\nu}\boldsymbol{\Sigma}_f^n\hat{\boldsymbol{\phi}}^n(\mathbf{r}), \tag{1}$$

where the hat (^) on the neutron flux denotes the homogeneous flux which is allowed to be discontinuous across the boundary of the node according to the equivalence theory.[4,5]

In contrast to the most nodal methods that solve the transverse-integrated equivalent one-dimensional diffusion equations, AFEN solves directly this three-dimensional diffusion equation. The solution of the diffusion equation (1) in the Cartesian coordinates can be expressed in matrix function form by

$$\begin{aligned}\hat{\boldsymbol{\phi}}^n(x,y,z)=\int_\Gamma\Big[&\sinh(\sqrt{\boldsymbol{\Lambda}^n}\boldsymbol{\tau}_1\cdot\mathbf{r})\{\mathbf{A}_0'(\boldsymbol{\tau}_1)+\boldsymbol{\tau}_2\cdot\mathbf{r}\,\mathbf{A}_1'(\boldsymbol{\tau}_1)+\boldsymbol{\tau}_3\cdot\mathbf{r}\,\mathbf{A}_2'(\boldsymbol{\tau}_1)+(\boldsymbol{\tau}_2\cdot\mathbf{r})(\boldsymbol{\tau}_3\cdot\mathbf{r})\,\mathbf{A}_3'(\boldsymbol{\tau}_1)\}\\&+\cosh(\sqrt{\boldsymbol{\Lambda}^n}\boldsymbol{\tau}_1\cdot\mathbf{r})\{\mathbf{B}_0'(\boldsymbol{\tau}_1)+\boldsymbol{\tau}_2\cdot\mathbf{r}\,\mathbf{B}_1'(\boldsymbol{\tau}_1)+\boldsymbol{\tau}_3\cdot\mathbf{r}\,\mathbf{B}_2'(\boldsymbol{\tau}_1)+(\boldsymbol{\tau}_2\cdot\mathbf{r})(\boldsymbol{\tau}_3\cdot\mathbf{r})\,\mathbf{B}_3'(\boldsymbol{\tau}_1)\}\Big]d\boldsymbol{\tau}_1,\end{aligned} \tag{2}$$

where

$$\boldsymbol{\Lambda}^n=\left(\mathbf{D}^n\right)^{-1}\left(\boldsymbol{\Sigma}^n-\frac{1}{k_{eff}}\boldsymbol{\nu}\boldsymbol{\Sigma}_f^n\right), \tag{3}$$

$\mathbf{r}$ = x$\mathbf{i}$+y$\mathbf{j}$+z$\mathbf{k}$ for unit vectors $\mathbf{i}$, $\mathbf{j}$, and $\mathbf{k}$ in x, y, and z directions, respectively,

$\boldsymbol{\tau}_i$ on Γ, $\boldsymbol{\tau}_i=\alpha_i\mathbf{i}+\beta_i\mathbf{j}+\gamma_i\mathbf{k}$, and $\alpha_i^2+\beta_i^2+\gamma_i^2=1$,

$\boldsymbol{\tau}_1\cdot\boldsymbol{\tau}_2=0$, $\boldsymbol{\tau}_2\cdot\boldsymbol{\tau}_3=0$, $\boldsymbol{\tau}_3\cdot\boldsymbol{\tau}_1=0$ for $\boldsymbol{\tau}_1\neq\boldsymbol{\tau}_2\neq\boldsymbol{\tau}_3$.

The terms $\mathbf{A}_i'$ and $\mathbf{B}_i'$ multiplied by $\boldsymbol{\tau}_i\cdot\mathbf{r}$ in Eq.(2) are transverse gradient basis functions. Evaluation of matrix functions in this equation is described in Ref.[6].

As in the original AFEN method, we choose nine $\boldsymbol{\tau}_1$'s so that they are evenly distributed 45 degrees apart on three unit circles on the x-y, y-z, and z-x planes, as follows:

$$(1,0,0),(0,1,0),(0,0,1),\left(\frac{\sqrt{2}}{2},\frac{\sqrt{2}}{2},0\right),\left(\frac{\sqrt{2}}{2},-\frac{\sqrt{2}}{2},0\right),\left(0,\frac{\sqrt{2}}{2},\frac{\sqrt{2}}{2}\right),\left(0,\frac{\sqrt{2}}{2},-\frac{\sqrt{2}}{2}\right),\left(\frac{\sqrt{2}}{2},0,\frac{\sqrt{2}}{2}\right),\left(-\frac{\sqrt{2}}{2},0,\frac{\sqrt{2}}{2}\right).$$

Noting that there are eight basis functions corresponding to each chosen $\boldsymbol{\tau}_1$, we can include total 72 basis functions satisfying the diffusion equations in the flux expansion.

We choose only 48 terms among the 72 terms and a constant term to expand the intranodal homogeneous flux in a node:

$$\hat{\boldsymbol{\phi}}^{n}(x,y,z) = \mathbf{E} + \boldsymbol{\varphi}^{n}(x,y,z) + \boldsymbol{\varphi}^{n}(y,z,x) + \boldsymbol{\varphi}^{n}(z,x,y), \tag{4}$$

where

$$\begin{aligned}\boldsymbol{\varphi}^{n}(x,y,z) = {} & \sinh\left(\sqrt{\boldsymbol{\Lambda}^{n}}\,x\right)\left\{\mathbf{A}_0^x + y\mathbf{A}_1^x + z\,\mathbf{A}_2^x + yz\,\mathbf{A}_3^x\right\} + \cosh\left(\sqrt{\boldsymbol{\Lambda}^{n}}\,x\right)\left\{\mathbf{B}_0^x + y\mathbf{B}_1^x + z\,\mathbf{B}_2^x + yz\,\mathbf{B}_3^x\right\} \\ & + \sinh\left(\frac{\sqrt{2\boldsymbol{\Lambda}^{n}}}{2}(x+y)\right)\left\{\mathbf{C}_{00}^x + z\mathbf{D}_{00}^x\right\} + \cosh\left(\frac{\sqrt{2\boldsymbol{\Lambda}^{n}}}{2}(x+y)\right)\left\{\mathbf{C}_{01}^x + z\mathbf{D}_{01}^x\right\} \\ & + \sinh\left(\frac{\sqrt{2\boldsymbol{\Lambda}^{n}}}{2}(x-y)\right)\left\{\mathbf{C}_{10}^x + z\mathbf{D}_{10}^x\right\} + \cosh\left(\frac{\sqrt{2\boldsymbol{\Lambda}^{n}}}{2}(x-y)\right)\left\{\mathbf{C}_{11}^x + z\mathbf{D}_{11}^x\right\}.\end{aligned} \tag{5}$$

The reason why the constant term **E** is introduced in the flux expansion and its function are described in Ref.[1].

The 49 coefficients in the flux expansion (5) are to be determined in terms of 49 nodal unknowns, that are composed of a node average flux, six interface fluxes, 18 interface moments, 12 edge fluxes, and 12 edge moments. For a three-dimensional node, it is very complicated to demonstrate the process of expressing all 49 coefficients. In a two-dimensional square node shown in Fig. 1, the equivalent flux expansion is given by

$$\begin{aligned}\hat{\boldsymbol{\phi}}^{n}(x,y) = {} & \mathbf{E} + \sinh\left(\sqrt{\boldsymbol{\Lambda}^{n}}\,x\right)\left\{\mathbf{A}_0^x + y\mathbf{A}_1^x\right\} + \cosh\left(\sqrt{\boldsymbol{\Lambda}^{n}}\,x\right)\left\{\mathbf{B}_0^x + y\mathbf{B}_1^x\right\} \\ & + \sinh\left(\sqrt{\boldsymbol{\Lambda}^{n}}\,y\right)\left\{\mathbf{A}_0^y + x\mathbf{A}_1^y\right\} + \cosh\left(\sqrt{\boldsymbol{\Lambda}^{n}}\,y\right)\left\{\mathbf{B}_0^y + x\mathbf{B}_1^y\right\} \\ & + \sinh\left(\frac{\sqrt{2\boldsymbol{\Lambda}^{n}}}{2}(x+y)\right)\mathbf{C}_{00}^x + \cosh\left(\frac{\sqrt{2\boldsymbol{\Lambda}^{n}}}{2}(x+y)\right)\mathbf{C}_{01}^x \\ & + \sinh\left(\frac{\sqrt{2\boldsymbol{\Lambda}^{n}}}{2}(x-y)\right)\mathbf{C}_{10}^x + \cosh\left(\frac{\sqrt{2\boldsymbol{\Lambda}^{n}}}{2}(x-y)\right)\mathbf{C}_{11}^x.\end{aligned} \tag{6}$$

This expansion contains only 13 terms whose coefficients are expressed into a node average flux, four interface fluxes, four interface flux moments, and four corner-point fluxes as follows:

$$\begin{aligned}&\bar{\hat{\boldsymbol{\phi}}}^{n} = \frac{1}{h^2}\int_{-\frac{h}{2}}^{\frac{h}{2}}\int_{-\frac{h}{2}}^{\frac{h}{2}} \hat{\boldsymbol{\phi}}(x,y)\,dy\,dx\ , && \hat{\boldsymbol{\phi}}_{11}^{n} = \hat{\boldsymbol{\phi}}^{n}\left(\frac{h}{2},\frac{h}{2}\right)\ , \\ &\tilde{\hat{\boldsymbol{\phi}}}_{x1}^{n} = \frac{1}{h}\int_{-\frac{h}{2}}^{\frac{h}{2}} \hat{\boldsymbol{\phi}}^{n}\left(\frac{h}{2},y\right)dy\ , && \tilde{\hat{\boldsymbol{\psi}}}_{x1}^{n} = \frac{1}{h}\int_{-\frac{h}{2}}^{\frac{h}{2}} \mathrm{w}(y)\,\hat{\boldsymbol{\phi}}^{n}\left(\frac{h}{2},y\right)dy\ ,\end{aligned} \tag{7}$$

where the subscripts on the nodal quantities refer to interfaces and corner points of the node in Fig. 1.

In Eq. (7), $\tilde{\hat{\boldsymbol{\psi}}}_{x1}^{n}$ is the flux moment defined at the interface x1 of node n, which is newly introduced by the adoption of the added expansion terms. The current moment corresponding to the flux moment (7) is also defined by

$$\tilde{\mathbf{j}}_{x0}^{n} = -\frac{\mathbf{D}^{n}}{h}\int_{-\frac{h}{2}}^{\frac{h}{2}} w(y)\frac{\partial}{\partial x}\hat{\boldsymbol{\phi}}^{n}(x,y)dy\Bigg|_{x=-\frac{h}{2}}. \tag{8}$$

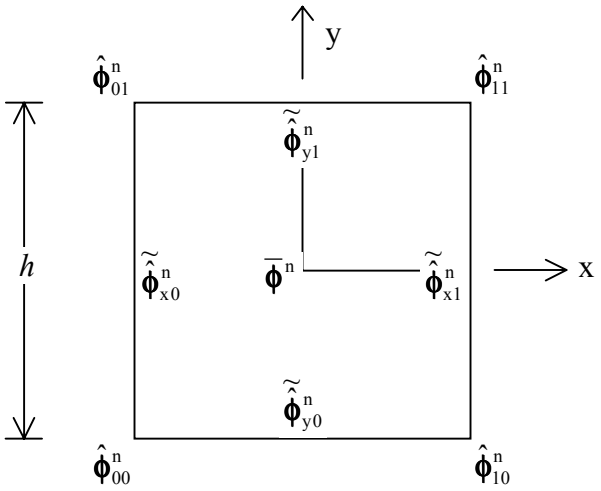

Figure 1. Geometry of Node n

Physically, since the flux and the current should be continuous at any point on an interface, this flux moment and the current moment should also be continuous across the interface.

In the definition of the flux moment and the current moment, w(y) is a weighting function given by an odd function of y. Two types of w(y), i.e., the step function and the linear function of y are examined as the weighting function in this paper:

$$\mathrm{w(y)} = \begin{cases} -1 & \text{for } \mathrm{y} < 0 \\ 1 & \text{for } \mathrm{y} \geq 0 \end{cases} \quad \text{and} \quad \mathrm{w(y)} = \mathrm{y}. \tag{9}$$

The step function was used in the group-theoretic nodal method[7] in which basis functions are equivalent to those in the original AFEN method.

Now the expansion coefficients are expressed in the nodal unknowns. For example, if we choose the linear function as a weighting function, $\mathbf{B}_0^x$ is given in terms of nodal unknowns as follows:

$$\begin{aligned}\mathbf{B}_0^x = &\left\{\mathbf{I} - \left(\frac{\sqrt{\boldsymbol{\Lambda}^{\mathrm{n}}}h}{2}\right)^{-1}\tanh\left(\frac{\sqrt{\boldsymbol{\Lambda}^{\mathrm{n}}}h}{2}\right)\right\}^{-1}\operatorname{sech}\left(\frac{\sqrt{\boldsymbol{\Lambda}^{\mathrm{n}}}h}{2}\right)\left[\left(\frac{1}{2}(\tilde{\tilde{\boldsymbol{\phi}}}_{x0}^{n} + \tilde{\tilde{\boldsymbol{\phi}}}_{x1}^{n}) - \bar{\boldsymbol{\phi}}^{\mathrm{n}}\right)\right. \\ &+\left\{2\boldsymbol{\Lambda}^{\mathrm{n}}h^2 + 4\sqrt{2\boldsymbol{\Lambda}^{\mathrm{n}}}\,h\,\sinh\left(\frac{\sqrt{\boldsymbol{\Lambda}^{\mathrm{n}}}h}{2}\right) + \left(16 + 4\boldsymbol{\Lambda}^{\mathrm{n}}h^2\right)\sinh^2\left(\frac{\sqrt{2\boldsymbol{\Lambda}^{\mathrm{n}}}h}{4}\right)\right\}^{-1} \\ &\left.\bullet\left(2\sqrt{2\boldsymbol{\Lambda}^{\mathrm{n}}}h\,\sinh\left(\frac{\sqrt{2\boldsymbol{\Lambda}^{\mathrm{n}}}h}{2}\right) - 16\sinh^2\left(\frac{\sqrt{2\boldsymbol{\Lambda}^{\mathrm{n}}}h}{4}\right)\right)\left(\frac{1}{4}\sum_{\mathrm{i,j}}\hat{\boldsymbol{\phi}}_{ij}^{n}\right)\right],\end{aligned} \tag{10}$$

where the indices i and j run over all points in the node, and

$$\delta\hat{\boldsymbol{\phi}}_{ij}^{n} = \hat{\boldsymbol{\phi}}_{ij}^{n} - \tilde{\hat{\boldsymbol{\phi}}}_{xi}^{n} - \tilde{\hat{\boldsymbol{\phi}}}_{yj}^{n} + \bar{\boldsymbol{\phi}}^{n}. \tag{11}$$

II.A.2 Nodal Coupling Equations

The nodal unknowns in the homogeneous flux expansions in a node are inter-coupled to the unknowns for neighboring nodes through the nodal coupling equations. Such coupling equations are composed of the ones to be solved for each type of the nodal unknowns. Since we use four types of nodal unknowns, we need four types of nodal coupling equations: the neutron balance equations for the node average fluxes, the interface current continuity equations for the interface fluxes, the interface current moment continuity equations for the interface current moments, and the leakage balance equations for the corner-point fluxes.

For example, expressing the current at the interface x0 of node n into

$$\begin{aligned}
\tilde{\mathbf{J}}_{x0}^{n} &= -\frac{\mathbf{D}^{n}}{h}\int_{-\frac{h}{2}}^{\frac{h}{2}} \frac{\partial\hat{\boldsymbol{\phi}}^{n}(x,y)}{\partial x}dy\Big|_{x=-\frac{h}{2}} \\
&= \mathbf{T}_{J1}^{n}\frac{1}{2}\left(\tilde{\tilde{\boldsymbol{\phi}}}_{x0}^{n} + \tilde{\tilde{\boldsymbol{\phi}}}_{x1}^{n}\right) + \mathbf{T}_{J2}^{n}\frac{1}{2}\left(\tilde{\tilde{\boldsymbol{\phi}}}_{x0}^{n} - \tilde{\tilde{\boldsymbol{\phi}}}_{x1}^{n}\right) + \mathbf{T}_{J3}^{n}\frac{1}{4}\left(\delta\hat{\boldsymbol{\phi}}_{00}^{n} + \delta\hat{\boldsymbol{\phi}}_{01}^{n} + \delta\hat{\boldsymbol{\phi}}_{10}^{n} + \delta\hat{\boldsymbol{\phi}}_{11}^{n}\right) \\
&\quad + \mathbf{T}_{J4}^{n}\frac{1}{4}\left(\delta\hat{\boldsymbol{\phi}}_{00}^{n} + \delta\hat{\boldsymbol{\phi}}_{01}^{n} - \delta\hat{\boldsymbol{\phi}}_{10}^{n} - \delta\hat{\boldsymbol{\phi}}_{11}^{n}\right) + \mathbf{T}_{J5}^{n}\frac{1}{2}\left(\tilde{\tilde{\boldsymbol{\psi}}}_{y0}^{n} + \tilde{\tilde{\boldsymbol{\psi}}}_{y1}^{n}\right) - \mathbf{T}_{J1}^{n}\boldsymbol{\phi}^{n},
\end{aligned} \tag{12}$$

the continuity equation at the interface between node i-1j and ij in Fig. 2 is given by

$$\begin{aligned}
&\frac{1}{2}\sum_{k=0,1}\left(\mathbf{T}_{J1}^{i-kj} - \mathbf{T}_{J2}^{i-kj} - \mathbf{T}_{J3}^{i-kj} + \mathbf{T}_{J4}^{i-kj}\right)\left(\tilde{\mathbf{F}}^{i-kj}\right)^{-1}\tilde{\boldsymbol{\phi}}_{i-2k+1j}^{x} + \frac{1}{2}\sum_{k=0,1}\left(\mathbf{T}_{J1}^{i-kj} + \mathbf{T}_{J2}^{i-kj} - \mathbf{T}_{J3}^{i-kj} - \mathbf{T}_{J4}^{i-kj}\right)\left(\tilde{\mathbf{F}}^{i-kj}\right)^{-1}\tilde{\boldsymbol{\phi}}_{ij}^{x} \\
&= -\frac{1}{4}\sum_{k=0,1}\left(\mathbf{T}_{J3}^{i-kj} - \mathbf{T}_{J4}^{i-kj}\right)\left(\mathbf{F}^{i-kj}\right)^{-1}\left(\boldsymbol{\phi}_{i-2k+1j+1} + \boldsymbol{\phi}_{i-2k+1j}\right) - \frac{1}{4}\sum_{k=0,1}\left(\mathbf{T}_{J3}^{i-kj} + \mathbf{T}_{J4}^{i-kj}\right)\left(\mathbf{F}^{i-kj}\right)^{-1}\left(\boldsymbol{\phi}_{ij+1} + \boldsymbol{\phi}_{ij}\right) \\
&\quad - \frac{1}{2}\sum_{k=0,1}\mathbf{T}_{J5}^{i-kj}\left(\tilde{\mathbf{F}}^{i-kj}\right)^{-1}\left(\tilde{\boldsymbol{\psi}}_{i-kj+1}^{y} + \tilde{\boldsymbol{\psi}}_{i-kj}^{y}\right) + \sum_{k=0,1}\mathbf{T}_{J1}^{i-1k}\boldsymbol{\phi}_{i-kj}.
\end{aligned} \tag{13}$$

where **T**'s are functions of k_{eff} and cross sections of the two nodes. This equation is a block tridiagonal matrix equation, which is easily solved for $\tilde{\boldsymbol{\phi}}_{ij}^{x}$.

The four types of nodal coupling equations are available for an iteration procedure. The conventional scheme consisting of two levels of iterations, i.e., inner iteration and outer iteration may be used.

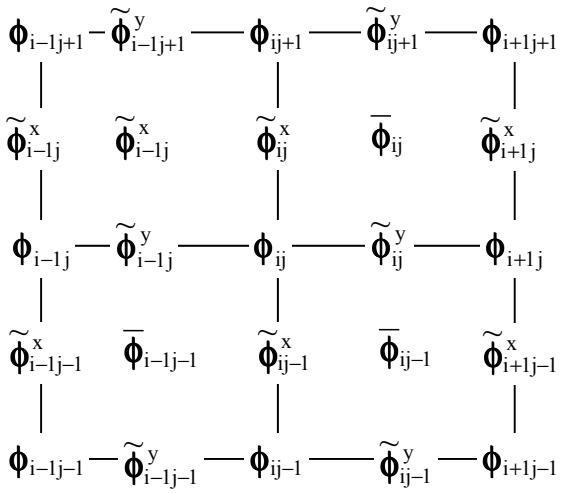

Figure 2. Geometry for the Derivation of Nodal Coupling Equations

II.B. Hexagonal Geometry

II.B.1 Intranodal Flux Expansion

To expand the intranodal homogeneous flux in a two-dimensional hexagonal node into analytic basis functions, we choose three τ_l's so that they are evenly distributed, 120 degrees rotated, in the unit circle on the x-y plane, and we set three coordinate systems, (x,y), (p,q) and (u,v) such that each x, p and u axis coincides with each of the three τ_l's.

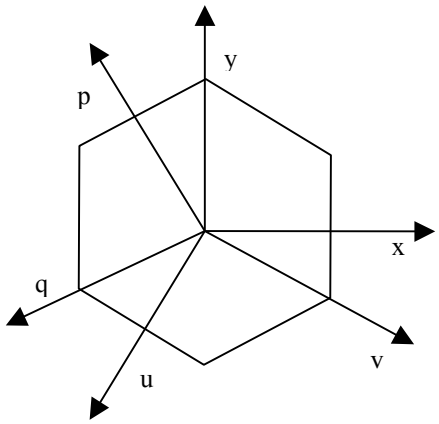

Figure 3. Coordinate Systems for the Hexagonal Node

Compared to that in the original AFEN method, the flux expansion in the refined method has the transverse gradient terms, which are hyperbolic functions multiplied by linear functions in the transverse direction to the hyperbolic functions. These transverse gradient functions, still satisfying the diffusion equation, are added to express the flux shape more accurately. For each chosen $\boldsymbol{\tau}_l$, there are six basis functions; four hyperbolic functions and the two transverse gradient functions. One of the three function sets for the corresponding coordinate systems is shown in Eq. (14):

$$\begin{aligned}\boldsymbol{\varphi}(x,y) = &\sinh\left(\sqrt{\boldsymbol{\Lambda}^{\mathrm{n}}}x\right)\left(\mathbf{A}_0^x + \mathbf{A}_1^x\, y\right) + \cosh\left(\sqrt{\boldsymbol{\Lambda}^{\mathrm{n}}}x\right)\left(\mathbf{B}_0^x + \mathbf{B}_1^x\, y\right) \\ &+ \sinh\left(\sqrt{\boldsymbol{\Lambda}^{\mathrm{n}}}y\right)\mathbf{A}_0^y + \cosh\left(\sqrt{\boldsymbol{\Lambda}^{\mathrm{n}}}y\right)\mathbf{B}_0^y ,\end{aligned} \tag{14}$$

With its two symmetric pairs in the (u,v) and the (p,q) coordinates and a constant, this function set is superposed to express the flux shape in the hexagonal node, thus results in 19 coefficients whereas the previous expansion in the rectangular node has 13 coefficients:

$$\hat{\boldsymbol{\phi}}^{\mathrm{n}} = \mathbf{E} + \boldsymbol{\varphi}(x,y) + \boldsymbol{\varphi}(p,q) + \boldsymbol{\varphi}(u,v) \ . \tag{15}$$

The 19 coefficients in the flux expansion are to be determined in terms of the nodal unknowns such as the node average flux, the interface fluxes, the interface flux moments and corner-point fluxes. These four kinds of nodal unknowns are defined in Eq. (16) and shown in Fig. 4. These 19 nodal unknowns are expressed by linear equations of the 19 flux expansion coefficients.

$$\begin{aligned}
&\bar{\hat{\boldsymbol{\phi}}} = \frac{8\sqrt{3}}{9h^2}\int_0^{\frac{\sqrt{3}}{2}h}\int_0^{-\frac{\sqrt{3}}{3}x+h}\hat{\boldsymbol{\phi}}(x,y)\,dy\,dx \ , && \hat{\boldsymbol{\phi}}_1^x = \hat{\boldsymbol{\phi}}^{\mathrm{n}}(0,h) \ , \\
&\tilde{\hat{\boldsymbol{\phi}}}_1^x = \frac{1}{h}\int_{-\frac{h}{2}}^{\frac{h}{2}}\hat{\boldsymbol{\phi}}^{\mathrm{n}}\left(\frac{\sqrt{3}}{2}h,y\right)dy \ , && \tilde{\hat{\boldsymbol{\psi}}}_1^x = \frac{1}{h}\int_{-\frac{h}{2}}^{\frac{h}{2}}\mathrm{w}(y)\,\hat{\boldsymbol{\phi}}^{\mathrm{n}}\left(\frac{\sqrt{3}}{2}h,y\right)dy \ ,
\end{aligned} \tag{16}$$

where w(y) is a weighting function for the flux moment. Two types of w(y), i.e., the step function and the linear function of y are also applicable for the hexagonal geometry.

The expression for one of the nodal unknowns, node average flux, is shown in Eq. (17) as an example,

$$\begin{aligned}
\bar{\hat{\boldsymbol{\phi}}}^{\mathrm{n}} &= \frac{8\sqrt{3}}{9h^2}\int_0^{\frac{\sqrt{3}}{2}h}\int_0^{-\frac{\sqrt{3}}{3}x+h}\hat{\boldsymbol{\phi}}^{\mathrm{n}}(x,y)\,dy\,dx \\
&= \mathbf{E} + \frac{4}{9\boldsymbol{\Lambda}^{\mathrm{n}}h^2}\left[6\left\{\cosh\left(\sqrt{\boldsymbol{\Lambda}^{\mathrm{n}}}h\right) - \cosh\left(\frac{\sqrt{\boldsymbol{\Lambda}^{\mathrm{n}}}h}{2}\right)\right\}\left\{\mathbf{B}_0^y + \mathbf{B}_0^v + \mathbf{B}_0^z\right\}\right. \\
&\quad \left. + \left\{4\sinh^2\left(\frac{\sqrt{3\boldsymbol{\Lambda}^{\mathrm{n}}}h}{4}\right) + \sqrt{3\boldsymbol{\Lambda}^{\mathrm{n}}}h\sinh\left(\frac{\sqrt{3\boldsymbol{\Lambda}^{\mathrm{n}}}h}{2}\right)\right\}\left\{\mathbf{B}_0^x + \mathbf{B}_0^u + \mathbf{B}_0^w\right\}\right] .
\end{aligned} \tag{17}$$

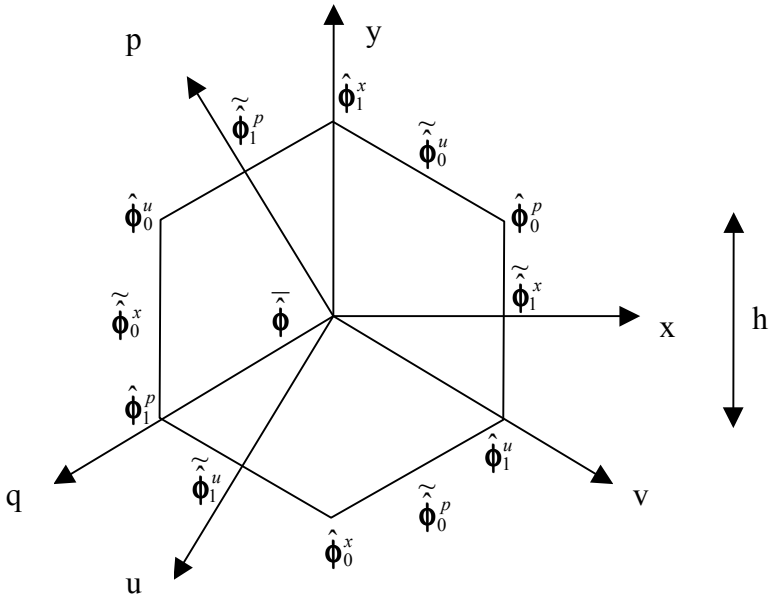

Figure 4. Coordinate Systems and Nodal Unknowns

Analogous expressions for the other 18 nodal unknowns together with Eq. (17) result in 19 simultaneous linear equations. The 19 flux expansion coefficients can be expressed by the nodal unknowns. For example,

$$\begin{aligned}\mathbf{A}_0^x = \mathbf{c}_1 &\left\{\tilde{\tilde{\hat{\boldsymbol{\phi}}}}_1^x - \tilde{\tilde{\hat{\boldsymbol{\phi}}}}_0^x + \tilde{\tilde{\hat{\boldsymbol{\phi}}}}_1^u - \tilde{\tilde{\hat{\boldsymbol{\phi}}}}_0^u + \tilde{\tilde{\hat{\boldsymbol{\phi}}}}_1^p - \tilde{\tilde{\hat{\boldsymbol{\phi}}}}_0^p\right\} \\ &+ \mathbf{c}_2\left\{\mathbf{2}\left(\tilde{\tilde{\hat{\boldsymbol{\phi}}}}_1^x - \tilde{\tilde{\hat{\boldsymbol{\phi}}}}_0^x\right) - \tilde{\tilde{\hat{\boldsymbol{\phi}}}}_1^u + \tilde{\tilde{\hat{\boldsymbol{\phi}}}}_0^u - \tilde{\tilde{\hat{\boldsymbol{\phi}}}}_1^p + \tilde{\tilde{\hat{\boldsymbol{\phi}}}}_0^p\right\} \\ &+ \mathbf{c}_3\left\{\hat{\boldsymbol{\phi}}_1^u - \hat{\boldsymbol{\phi}}_0^u - \hat{\boldsymbol{\phi}}_1^p + \hat{\boldsymbol{\phi}}_0^p\right\} + \mathbf{c}_4\left\{\tilde{\tilde{\boldsymbol{\psi}}}_1^u + \tilde{\tilde{\boldsymbol{\psi}}}_0^u - \tilde{\tilde{\boldsymbol{\psi}}}_1^p - \tilde{\tilde{\boldsymbol{\psi}}}_0^p\right\}.\end{aligned} \tag{18}$$

where $\mathbf{c}_1$, $\mathbf{c}_2$, $\mathbf{c}_3$ and $\mathbf{c}_4$ are constant matrices for the node.

II.B.2 Nodal Coupling Equations

The nodal coupling equations in the hexagonal node are derived also by considering the similar conditions to the rectangular case. These conditions are composed of the nodal neutron balance condition in node I, the current and the current moment continuity conditions across the interface between nodes I and II, and the leakage balance equation around the corner point shared by the three nodes, I, II, and III in Figure 5. Among them, the current moment continuity condition across the interface between nodes I and II in Figure 5 is given by

$$\tilde{\hat{\mathbf{j}}}_{x1}^{I} = -\frac{\mathbf{D}^{I}}{h}\int_{-\frac{h}{2}}^{\frac{h}{2}} w(y)\frac{\partial}{\partial x}\hat{\boldsymbol{\phi}}^{I}(x,y)dy\Bigg|_{x=\frac{\sqrt{3}}{2}h} = -\frac{\mathbf{D}^{II}}{h}\int_{-\frac{h}{2}}^{\frac{h}{2}} w(y)\frac{\partial}{\partial x}\hat{\boldsymbol{\phi}}^{II}(x,y)dy\Bigg|_{x=-\frac{\sqrt{3}}{2}h} = \tilde{\hat{\mathbf{j}}}_{x0}^{II}\ . \tag{19}$$

This provides the nodal coupling equation to be solved for the flux moment at the interface:

$$\begin{aligned}
&\mathbf{T}_L^I\tilde{\boldsymbol{\psi}}_4 + \left(\mathbf{T}_C^I + \mathbf{T}_C^{II}\right)\tilde{\boldsymbol{\psi}}_1 + \mathbf{T}_R^{II}\tilde{\boldsymbol{\psi}}_7 \\
&= \mathbf{T}_1^I\left(\tilde{\boldsymbol{\psi}}_6 + \tilde{\boldsymbol{\psi}}_1\right) + \mathbf{T}_2^I\left(\tilde{\boldsymbol{\psi}}_3 + \tilde{\boldsymbol{\psi}}_5\right) + \mathbf{T}_3^I\left(\tilde{\boldsymbol{\phi}}_2 + \tilde{\boldsymbol{\phi}}_3\right) + \mathbf{T}_4^I\left(\tilde{\boldsymbol{\phi}}_5 + \tilde{\boldsymbol{\phi}}_6\right) + \mathbf{T}_5^I\left(\tilde{\boldsymbol{\phi}}_1 + \tilde{\boldsymbol{\phi}}_4\right) \\
&+ \mathbf{T}_6^I\left(\boldsymbol{\phi}_1 + \boldsymbol{\phi}_3\right) + \mathbf{T}_7^I\left(\boldsymbol{\phi}_4 + \boldsymbol{\phi}_6\right) + \mathbf{T}_8^I\left(\boldsymbol{\phi}_2 - \boldsymbol{\phi}_5\right) + \mathbf{e}^{II}\ ,
\end{aligned} \tag{20}$$

where $\mathbf{T}_i^I$'s are constant matrices whose elements depend on k_{eff} and group constants of the node I, and $\mathbf{e}^{II}$ is expressed in terms containing the node average flux , the u- and p-direction interface fluxes, moments, and corner-point fluxes of the adjacent node II. This block tridiagonal matrix is solved for the interface flux moment $\tilde{\boldsymbol{\psi}}_1$.

This coupling equation for the flux moment and the other coupling equations for the corresponding nodal unknowns are also derived similarly and these nodal coupling equations are solved by an iterative procedure.

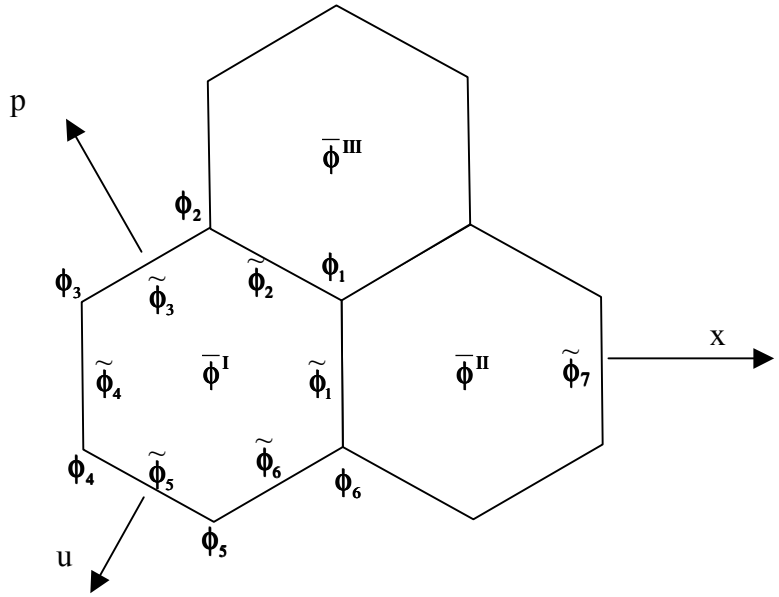

Figure 5. Geometry for the Derivation of Nodal Coupling Equations

III. Numerical Results and Discussion

Choosing the benchmark problems to test the refined AFEN method developed here is very careful, because the original AFEN method against which the refined method should show its accuracy improvement is so accurate for most problems. The problems with the explicit baffle and reflector model are not adequate for this purpose because its accuracy improvement could be hidden behind the relatively large errors caused by the baffle/reflector homogenization. Choosing the problems with smooth flux distribution is not good either to show the relative superiority of such a sophisticated method as the AFEN method.

The C5 configuration of the OECD-L336 problem[8] in rectangular geometry and the VVER-440 problem[9] in hexagonal geometry do not have a baffle region but they exhibit significant flux changes over the core volumes.

III.A. OECD-L336 Problem

The fuel assemblies in the C5 configuration of the OECD-L336 problem have different types of 17x17 pin-cells and were homogenized by the single-assembly calculations with the zero current boundary condition. The fine-mesh VENTURE[10] calculation was performed to provide the reference solution, after replacing the heterogeneous fuel assemblies with the homogeneous fuel assemblies. This is to see the performance of the refined method clearly by excluding the homogenization error.

In Fig. 6, the nodal unknowns and the effective multiplication factors calculated by three nodal methods were compared with those of the fine-mesh VENTURE calculation. The first calculation was performed by the original AFEN method. The second one was by the method that uses the interface flux moments as nodal unknowns instead of the corner-point fluxes in the original AFEN method (and less the flux expansion terms with $\mathbf{C}_{ij}$ in Eq.(6)). The third method uses both the interface flux moments and the corner-point fluxes as unknowns. The linear weighting function is used to define the flux moment for the latter two calculations, because we could not see any significant difference between the results using the step weighting function and the linear weighting function. As expected from the fact that the number of conditions constraining the intranodal flux distribution is unchanged, it cannot be easily judged which one is better between the original AFEN method and the second method using the interface moments only. This shows that there is no accuracy degradation in substituting the corner-point fluxes with the interface moments. It is also shown in the figure that the refined AFEN method taking both the corner-point fluxes and the interface moments reduces consistently the errors in the effective multiplication factor and the flux distribution. The computing times for the three different nodal calculations were not compared, because this problem is too small to require measurable computing times.

The original AFEN method shows good accuracy in predicting the flux distribution, in spite of the steep flux change in the region near the interface between the uranium-oxide fuel assembly and the mixed-oxide fuel assembly and the interface between fuel and reflector. Therefore there is not much need to improve the accuracy per se of the original AFEN method. But the other salient feature of the refined AFEN method would rather be its adaptability than its accuracy

improvement, as indicated in the introduction section. The method that replaces the corner-point fluxes with the interface flux moments can easily be adopted into the existing nodal codes with interface nodal unknowns only and may fit better for the non-linear iterative scheme based on two-node problems.

III.B. VVER-440 Problem

The core is of VVER-440[9] type with 25 assemblies across the core diameter as shown in Fig. 7. There are 7 control rod assemblies inserted and a layer of reflector assemblies is on the boundary of the core. The zero flux boundary condition was applied instead of the vacuum boundary condition given in the original problem. In VVER-440, the control rods are not inserted into the fuel assemblies, rather push out the fuel assemblies beneath them. Once inserted in the core, the control rod assemblies replace fuel assemblies, giving rise to steep flux gradients on the interfaces between a control rod assembly and the neighboring fuel assemblies. The assembly homogenized cross sections are directly quoted from the reference[9]. The reference solution is obtained by the VENTURE fine-mesh calculation with triangular meshes.

In Fig. 7, the assembly-wise relative powers of the three nodal calculations were compared with those of the reference calculation: the first one calculated by the original AFEN method, the second one calculated by the refined AFEN method which replaces the corner-point fluxes with the flux moments (and less the flux expansion terms with $\mathbf{A}_0^y$ and $\mathbf{B}_0^y$ in Eq.(14)), and the third one calculated by the refined AFEN method which uses both the corner-point fluxes and the flux moments. Again the linear weighting function is used in the definition of the flux moment. In the case of OECD-L336, the AFEN method with flux moments instead of corner-point fluxes was shown to be comparable in accuracy to the original AFEN method. But in this VVER-440 problem a great reduction in error of assembly powers was achieved by the refined AFEN method which replaces the corner-point fluxes with the flux moments. Even though this refined AFEN method has the same number of unknowns compared to the original AFEN method, the reduction of error is very large and the computing time is less than half of that of the original AFEN method. This can be explained by the fact that the inclusion of transverse gradient basis functions and the interface flux moments can describe more accurately the large flux gradients near the control rod assemblies and their neighboring assemblies, and that the continuity condition of the flux moments at the assembly boundaries is a more “global” constraint than the corner-points leakage balance condition because the former is related to the flux distributions along the boundaries whereas the latter is related only to the flux distribution near the points. The refined AFEN method which uses both the corner-point fluxes and the flux moments provides even more accurate result than the refined AFEN method without corner-point fluxes, and it does so with practically no increase of the computing time from that of the original AFEN method. This good performance of the refined AFEN method with flux moments brings us strong motivation of its application to the hexagonal reactor analysis.

IV. Conclusions

A refinement of the AFEN method has been performed by increasing the number of flux expansion terms in the manner that the original expansion basis functions are combined with the transverse-direction linear functions. In this manner, the added terms can render the flux expansion more complete and be kept to still satisfy the diffusion equation at any point in the node. The flux moments introduced at the interfaces provide the constraints required additionally by these added terms. The interface flux moments are defined by the average values of the fluxes weighted by odd functions in the parallel directions to the interface. Since the refined flux expansion also satisfies the diffusion equation and the additional constraints are applied, the salient feature of the original AFEN method is even more enforced in the refined method.

The refined AFEN method was tested against a mixed-oxide (MOX) fuel problem in rectangular geometry and a severely rodded problem in hexagonal geometry. The results show that the method improves not only the accuracy in predicting the homogeneous flux distribution and the effective multiplication factor but also the computing time. In the hexagonal geometry, these improvements are more conspicuous.

Since the original AFEN method is accurate enough for most applications, the other salient feature of the refined AFEN method would rather be its adaptability than its accuracy improvement. Maintaining the accuracy, this method can replace the corner-point fluxes with the interface moments so that the method may easily be implemented into the existing nodal codes that do not use the corner-point fluxes as unknowns. It may fit better for the non-linear scheme based on two-node problems that are solved for the interface quantities and is expected to show better performance.

References

1. Jae Man Noh and Nam Zin Cho, "A New Approach of Analytic Basis Function Expansion to Neutron Diffusion Nodal Calculation," *Nucl. Sci. Eng.*, **116**, 165 (1994).
2. Nam Zin Cho and Jae Man Noh, "Analytic Function Expansion Nodal Method for Hexagonal Geometry," *Nucl. Sci. Eng.*, **121**, 245 (1995).
3. Nam Zin Cho, Yong Hee Kim, and Keon Woo Park, “Extension of Analytic Function Expansion Nodal Method to Multigroup Problems in Hexagonal-Z Geometry,” *Nucl. Sci. Eng.*, **126**, 35 (1997).
4. K. Koebke, "A New Approach to Homogenization and Group Condensation," *Proc. IAEA Technical Committee Mtg.*, Lugano, Switzerland, November 1978, IAEA-TECDOC 231, p.303, International Atomic Energy Agency (1978).
5. K. S. Smith, "Spatial Homogenization Methods for Light Water Reactor Analysis," PhD Thesis, Massachusetts Institute of Technology (1980).
6. Jae Man Noh, et al., "A General Approach to Multigroup Extension of the Analytic Function Expansion Nodal Method Based on Matrix Function Theory," *Proc. 1996 Joint Intl. Conf.*

Mathematical Methods and Super Computing for Nuclear Applications, Saratoga Springs, New York, Octorber 6-10, 1997, Vol. **1**, p. 144, American Nuclear Society (1997).
7. S. Zhang and Z. Xie, “A New Nodal Method Based on Group Theory for the Multigroup Diffusion Calculation in Hexagonal Geometry,” *Proc. Int. Conf. on the Physics of Nuclear Science and Technology,* Long Island, New York, October 5-8, 1998, Vol. 2, p. 986, American Nuclear Society (1998).
8. J. C. Lefebvre, J. Mondot, and J. P. West, "Benchmark Calculations of Power Distribution within Assemblies," NEACRP-L-336, Organization for Economic Cooperation and Development (1991).
9. Y. A. Chao and Y. A. Shatilla, "Conformal Mapping and Hexagonal Nodal Methods-II; Implementation in the ANC-H Code,” *Nucl. Sci. Eng.*, **121**, 210 (1995).
10. D. R. Vondy, et al., “VENTURE: A Code Block for Solving Multigroup Neutronic Problems Applying the Finite-Difference Diffusion Theory Approximation to Neutron Transport – Version II,” ORNL-5062/R1, Oak Ridge National Laboratory (1977).

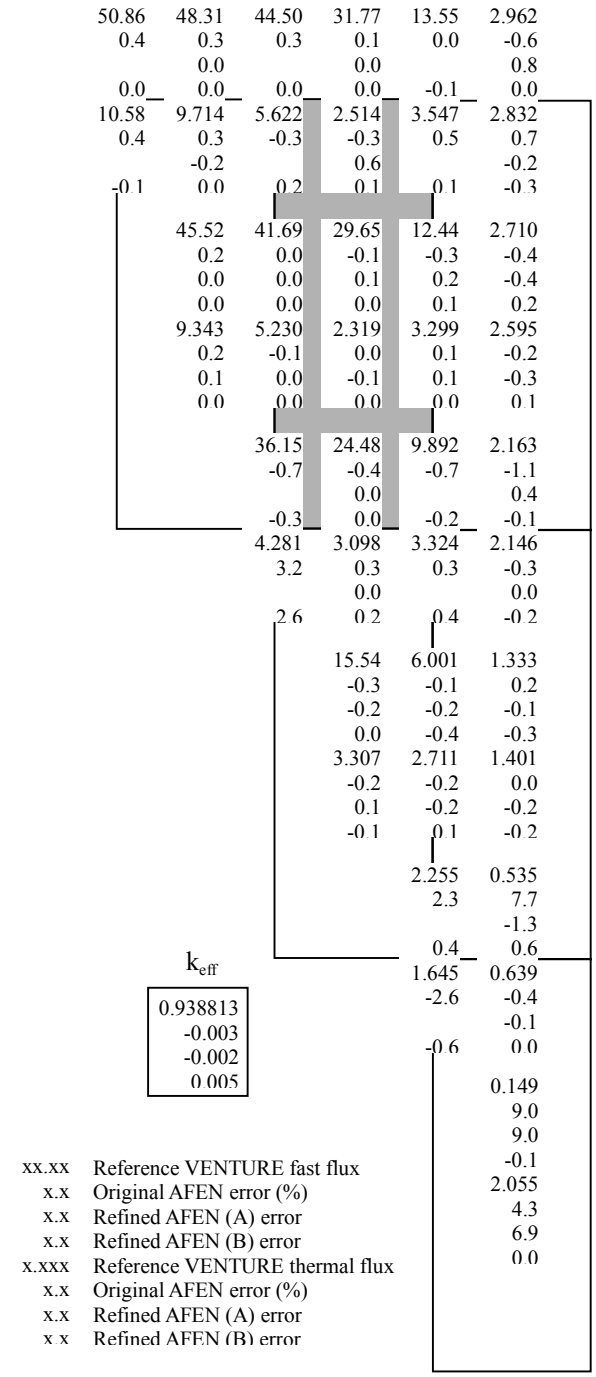

Mesh size of reference VENTURE calculation : 1.26 cm; mesh size of nodal calculation : 21.45 cm.
The refined AFEN (A) uses the interface moments instead of the corner-point fluxes as unknowns.
The refined AFEN (B) uses both the interface moments and the corner-point fluxes as unknowns.
Shaded area denotes an MOX assembly.

Figure 6. Results of OECD-L336 Benchmark Problem

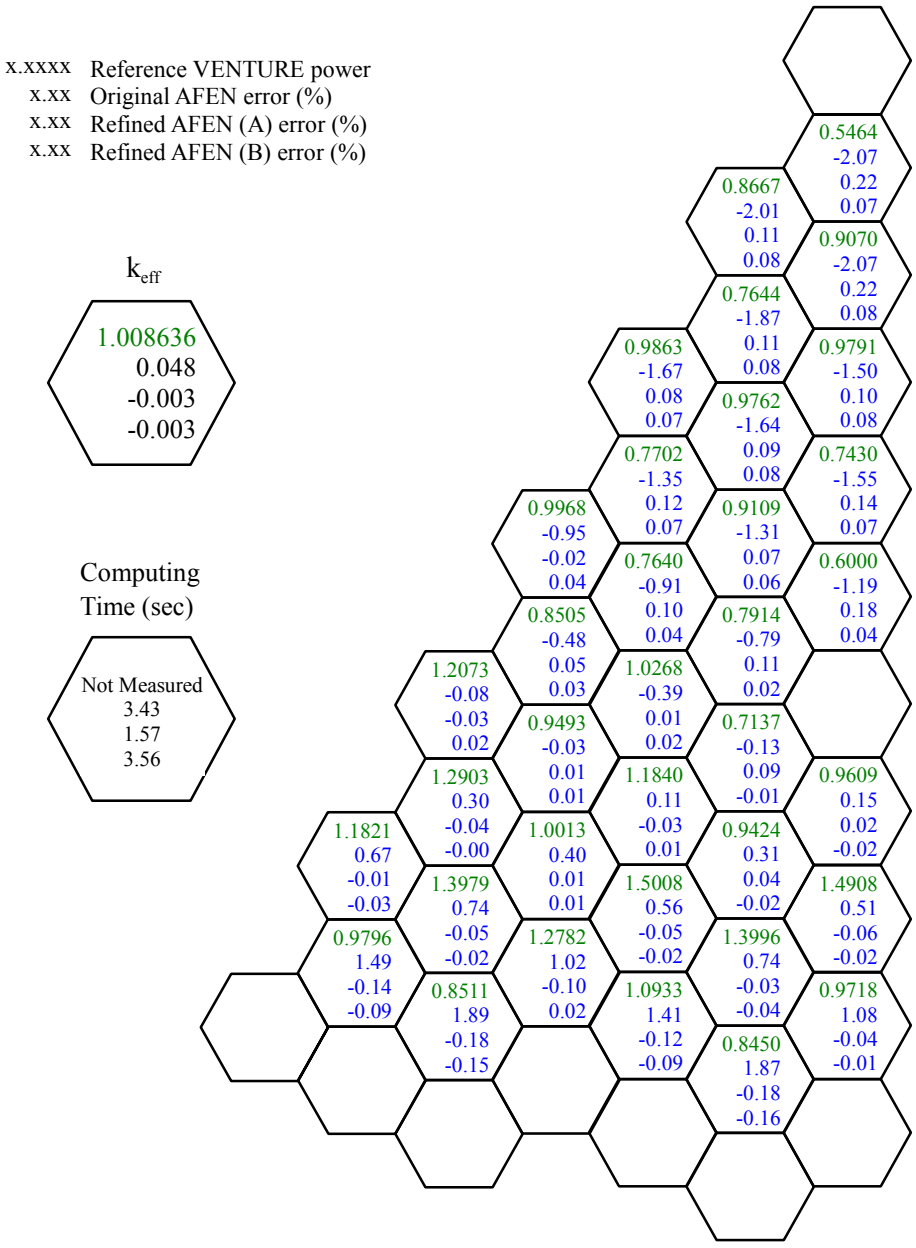

The number of meshes per assembly in the reference VENTURE calculation : 1536 triangles
The refined AFEN (A) uses the interface moments instead of the corner-point fluxes as unknowns.
The refined AFEN (B) uses both the interface moments and the corner-point fluxes as unknowns.
The computing time is measured on a Pentium-II PC.

Figure 7. Results of VVER-440 Benchmark Problem (1/12 Core)